Experimental Evaluation of Corrosion for Aluminum Alloy in Aerated NaCl Solutions under Turbulent Hydrodynamic Conditions

Ghulamullah Kakar[1], Faisal Mushtaq[1], Saeedullah Jan Mandokhail[2], Mohammad Siddique[1], Ali Nawaz Mengal[3]

[1]Department of Chemical Engineering, [2]Department of Civil Engineering, [3]Department of Petroleum and Gas Engineering, Balochistan University of Information Technology, Engineering and Management Sciences, Quetta, Pakistan

Abstract

The application of electrochemical impedance spectroscopy (EIS) and potentiodynamic polarization measurement were employed for the evolution of corrosion of aluminum alloy (6262) in artificial sea water under the turbulent flow conditions. The flow condition experiments were simulated using rotating cylinder electrode (RCE). The obtained results showed that enhancing the incremental fluid flow velocity, a significant change were occurred in corrosion reaction mechanism and improvement of the corrosion kinetic of the system were also been observed. By increasing the fluid flow velocity, there is an increase in the limiting current. This result conclude the presence of a mixed control on the corrosion process associated with the formation as well as stabilization of obtained corrosion product layers on the investigated electrode surface.

Keywords: Aluminum Alloy 6262; SEM; Corrosion Products; Flow Velocity Condition

Corresponding author's email: *ghulamullah@buitms.edu.pk*

INTRODUCTION

Aluminum and its alloys are widely used in a variety of industrial and domestic applications including: chemical reaction vessels, containers, electronic devices, aviation, chemical batteries, pipes and household appliances. Aluminum is an important material not only for its low cost, low density, favorable mechanical properties and high energy density but also have an excellent corrosion resistance in various aggressive solutions (Musa et al., 2010). In industrial processes, where the processes are operated at elevated conditions of temperature, pressure and high flow velocities, there are some possible consequences of corrosion attack in the pipelines and downstream process equipment. In order to overcome these circumstances, researchers are focused the effect of such process conditions including: temperature, flow velocities and pressure upsetting the rate of corrosion (Foley, 1986; Zhang et al., 2008; Ashassi-Sorkhabia et al., 2006).

Aluminum has the ability to resist corrosion in various acidic and alkaline media due to the formation of natural oxide layer on its surface, therefore, reduces the rate of corrosion to a satisfactory level. At a laboratory level, the internal corrosion caused by the hydrodynamic conditions are mostly difficult to simulate. In order to reproduce some specific operating conditions at laboratory level, a variety of devices like rotating disk electrodes, rotary cage with flow loop and jet impingement, have been developed for this particular purpose (Klapper et al., 2008). The employment of Rotating Cylinder Electrode (RCE) facilitates this type of simulations for donating important advantages.

The aim of this study was to investigate the corrosion mechanism of aluminum alloy 6262 in sea water (3.5 % NaCl solution) under the various conditions of flow rates. The electrochemical measurements including potentiodynamic polarization, electrochemical impedance spectroscopy (SEM) and scanning electron microscope were utilized in this study.

MATERIALS AND METHODS

In this study, the aluminum alloy (6262) was used as working electrode with elemental composition shown in Table 1. The working electrode was initially abraded mechanically using silicon Carbide/emery papers ranging from No. 400, 600, 800, 1200 and 1500 until a smooth surface appears, then washed with deionized water, followed by degreasing with ethanol and CCl4, and finally dried in desiccator before immersion into the test solution. The rotating cylinder electrode (RCE) was connected with a Gamry Potentiostat/Galvanostat/ ZRA instrument, model AFMSRCEP rotator, having a dimensions of 0.78 cm length, 1.2 cm diameter and

expose surface area of 2.94 cm2. The experiments were performed at flow velocities of 400, 800, 1200, 1600 and 2000 rpm at 40○C in aerated 3.5% NaCl solution. A water jacket glass cell with a capacity of 175 ml consisting of three electrodes including: working electrode, counter electrode and reference electrodes was utilized. The latter was a saturated calomel electrode (SCE). The measurements were carried out in aerated 3.5% NaCl test solution. All the test solutions were freshly prepared from analytical grade chemical reagents. For each test, a freshly prepared solution and cleaned set of electrodes were used.

Table 1: Composition of aluminum alloy (6262)

Elements	Contents, wt.%
Si	0.4
Fe	0.7
Cu	0.15
Mn	0.15
Ti	0.15
Zn	0.25
Pb	0.4
Bi	0.4
Al	Remainder

The relations for Reynolds number and conversion into linear velocity for a rotating cylinder electrode with outer diameter was given in equation 1 and 2 respectively (Schmitt and Bakalli, 2006).

$$N_{Re} = (U \cdot d)/v \quad (1)$$

$$U = (\pi . d . F)/60 \quad (2)$$

Where, U is the Kinematic viscosity of the test solution (cm^2/sec), v stands for flow velocity ($cm\ s^{-1}$), F is flow velocity in rpm and d denoting outer diameter (m) of rotating electrode. It is generally considered that, a rotating cylinder, the values of Reynolds number greater than 200, are considered to be a turbulent flow (Silverman, 2004). In the present study, the obtained values of Reynolds number values are tabulated in Table 2, which proves that the experiments were performed under the conditions of turbulent flow in brine solution.

Table 2: The values of Reynold's number for various flow velocities in 3.5 % NaCl at 40 ^{0}C

rpm	U ($m\ sec^{-1}$)	V ($m\ sec^{-2}$)	N_{Re}
400	25.13	0.00659	4577
800	50.26	0.00659	9155
1200	75.39	0.00659	13735
1600	100.53	0.00659	18313
2000	125.66	0.00659	22891

The surface morphological images of each investigated Aluminum alloy (6262) specimens were studied by mechanically abraded as received and after immersion into 3.5 % NaCl solution at 2000 rpm at 40 ^{o}C by

employing a JEOL JSM-840A scanning electron microscope at an accelerating voltage of 10 KeV. The electrodes immersion time for SEM analysis was 6 hours.

RESULTS AND DISCUSSION

Open Circuit Potential with rpm measurement

Fig. 2 represents the variations in OCP of aluminum alloy electrode 6262 and was monitored carefully at various flow conditions and at a constant temperature of 35 °C in 3.5 % NaCl solution. The significance of the anode potential is that more negative potential and greater the anode output, quicker rate of the polarization of the steel to which the anode is attached, greater the current output and greater the consumption of the anode (Gabe, 1974). It was observed that, the potential of the aluminum alloy (6262) electrode moves rapidly in the positive direction up to 1200 rpm, and later on a constant and steady potential up to 2000 rpm was recorded. As a consequence, the corrosion rate of aluminum alloy (6262) increasing due to the fracture and damage of oxide layer at the interface. Moreover, the protection of steel structure functioning as cathode is saline medium to be protected.

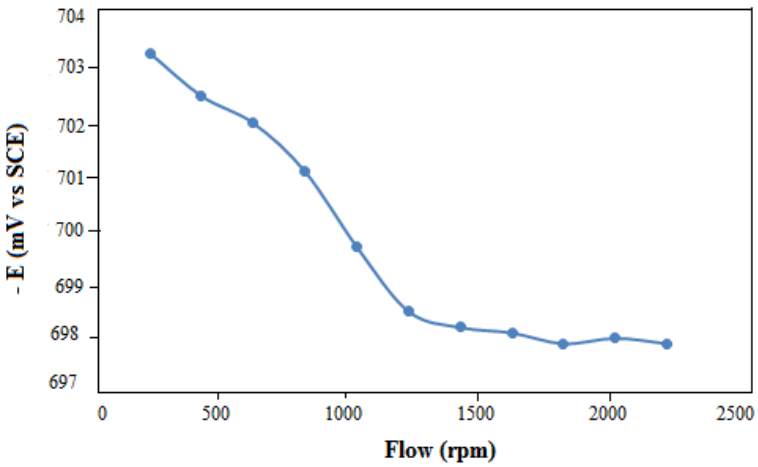

Figure 1: The change in OCP as a function of flow velocity for Aluminum alloy (6262) in 3.5 % NaCl solution at 40 °C

Potentiodynamic polarization

Potentiodynamic polarizations were carried out at 40 °C at different rotation rates. The polarization curves at different rotation were shown in Fig. 2.

It has been observed that there is a clear incremental increase in limiting current density (I_L), which is attributed to an oxygen diffusivity improvement, benefiting the mass transfer process (Fig. 2). In addition, corrosion on metal in the presence of oxygen is a mass transfer controlled process limited by the oxygen-transport at the reaction interface from the bulk solution. Moreover, the presence of limiting current density at the cathodic portion of the polarization curves reveal that the kinetic mechanism of the corrosion process was controlled by diffusion reaction. The values of I_L was determined carried out by means of graphical approach of the polarization curves and the attained values are presented in Table 3.

Electrochemical Impedance spectroscopy measurements

The Nyquist impedance plots at 35 °C under different rotation rates are presented in Figs 3. The formation of single depressed semicircles, the absence of the Warburg impedance behavior, as well as the presence of a loop at the low frequencies was characteristic of the obtained impedance spectra. The presence of a loop at the low frequencies has been attributed by some authors to changes in the corrosion kinetics of the electrochemical system during the EIS measurements, which is undeniable because the permanent effect of the wall shear stresses on the corrosion product layers observed covering the electrode surface. On the other hand, the depression of the impedance spectra has yet not been well understood and its physical origin

are still not clear (Cottis and Turgoose, 1999). However, some authors have related this special feature of the impedance spectra with metal dissolution under corrosion product films and the oxygen reduction within these porous oxide layers (Juettner et al., 1988).

From the Fig. 3, it is clear that the a clear reduction of the polarization resistance achieved from the analysis of the impedance spectra (R_p) against an increase of the flow velocity was observed, confirming the observed behavior in the polarization curves for the limiting current density where the corrosion rate improved with the flow velocity. The polarization resistance values (R_p) values are listed in Table 3.

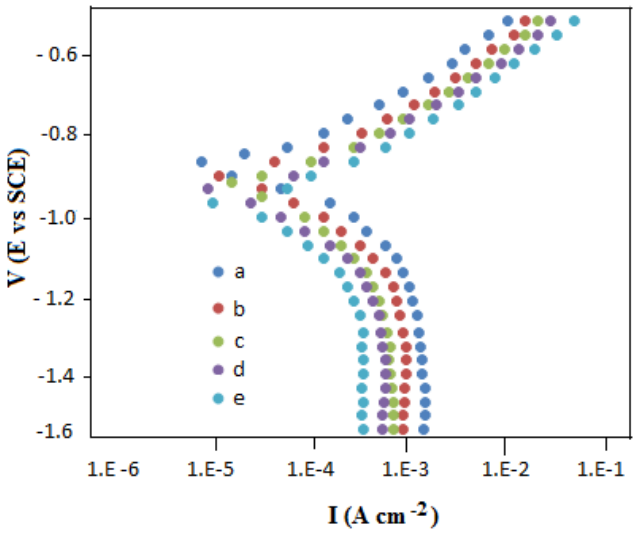

Figure 2: Potentiodynamic polarization curves for aluminum alloy (6262) in 3.5% NaCl solution and at 40 °C with different rpm: (a) 400, (b), 800 and (c) 1200, (d) 1600, (e) 2000

Table 3: Electrochemical parameters for aluminum alloy (6262) for various flow velocities in 3.5% at 40°C

Rotation (rpm)	E_{corr} (mV)	B_a (V/dec)	I_{corr} (μA cm^{-2})	I_L (μ A cm^{-2})	R_P (ohm cm^2)
400	706.3	0.0275	253	211	312.7
800	701.2	0.0284	416	441	203.2
1200	698.7	0.0341	789	806	106.4
1600	697.3	0.0601	1094	992	72.1
2000	695.9	0.0622	1132	1097	52.3

SEM analysis

SEM imaging was executed to establish a relation between the experimental parameters and the morphology of the aluminum alloy (6262) surface. Fig.4(a) signifies the surface image of the abraded sample before immersion in 3.5 % NaCl solution, whereas Fig. 4 (b) represent the image of Aluminum alloy (6262) surface at a flow velocity of 2000 rpm respectively. It can be observed that as-received Aluminum alloy (6262) Fig. 4(a), exhibits a smooth and uniform surface morphology. However, the immersion of Aluminum alloy (6262) into saline and dynamic environment (2000 rpm), there are some visible cracking and pitting marks on the surface are due to the formation of corrosion products and attack of the aggressive solution indicating reduced corrosion resistance.

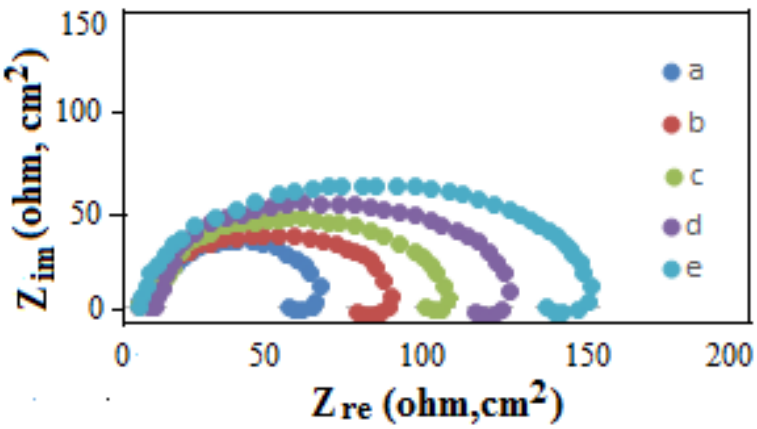

Figure 3: Nyquist plots for Aluminum alloy (6262) in 3.5% NaCl solution at 35 °C and with different rpm: (a) 2000, (b), 1600 and (c) 1200 (d) 800, (e) 400

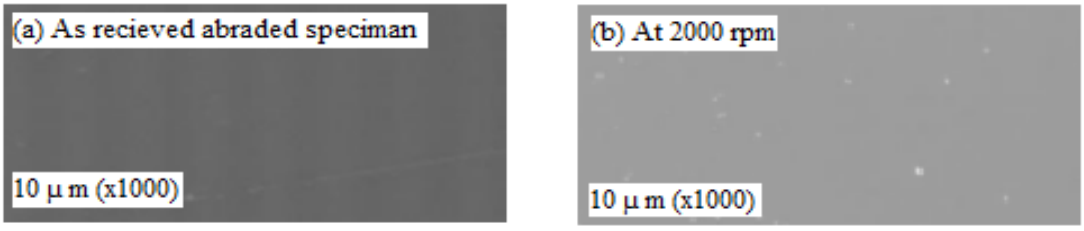

Figure 4: SEM morphology for Aluminum alloy (6262) before and after immersion into 3.5 % NaCl solution at 40 °C

CONCLUSION

Corrosion kinetics of the aluminum alloy (6262) in a solution of 3.5 % NaCl saturated with air was ominously affected by flow velocity and increasing Reynold number. Moreover, the limiting current density (I_L) was found increased with incrementally increase in flow velocity. This behavior was offered to the presence of a mixed type of control on the corrosion process related with the formation of thin corrosion product layers functioning as barrier for the flow of electrons on the electrode surface. More interestingly, the obtained results for corrosion rate and polarization resistance were found increased and by an incremental decrease in the liquid flow velocity, respectively.

REFERENCES

- Musa AY, Mohamad AB, Kadhum AAH, Takriff MS, Daud AR, Kamarudin SK. (2010). Inhibition of aluminum alloy 2024 corrosion by 4-amino-5-phenyl-4H-1, 2, 4-trizole-3-thiol in highly sulfuric acid solution. Advanced Materials Research 93-94: 354 -357.

- Foley RT. (1986). Localized Corrosion of Aluminum Alloys—A Review. CORROSION 42(5):277-288.

- Zhang F, Zhao L, Chen H, Xu S, Evans DG, Duan X. (2008). Corrosion Resistance of Superhydrophobic Layered Double Hydroxide Films on Aluminum. Angew. Chem. Int. 47:2466 –2469.

- Ashassi-Sorkhabia H, Shabanib B, Aligholipoura B, Seifzadehab D. (2006). The effect of some Schiff bases on the corrosion of aluminum in hydrochloric acid solution. Applied Surface Science 252(12):4039-4047.

- Klapper HS, Laverde DVasquez C. (2008). Evaluation of the corrosion of UNS G10200 steel in aerated brines under hydrodynamic conditions. Corrosion Science 50(9):2718-2723.
- Schmitt G, Bakalli M. (2006). A critical review of measuring techniques for corrosion rates under flow conditions. NACE International, San Diego, California, PP 27.
- Silverman DC. (2004). The rotating cylinder electrode for examining velocity-sensitive corrosion- a review. Corrosion 60(11):1003-1023
- Gabe DR. (1974). The rotating cylinder electrode. Journal of Applied Electrochemistry 4: 91-108.
- Cottis R, Turgoose S. (1999). Electrochemical Impedance and Noise. Corrosion Testing Made Easy, (Syrett, B.C, Series Editor), NACE International, Houston, TX, 1999
- Juettner K, Lorenz W, Kendig M, Mansfeld F. (1988). Electrochemical Impedance Spectroscopy on 3D Inhomogeneous Surfaces Corrosion in Neutral Aerated Solutions. Journal of the Electrochemical Society 135(2): 332-339.